Proceedings of DETC'02
ASME 2002 Design Engineering Technical Conferences and Computers and Information in Engineering Conference
Montreal, CANADA, September 29-October 2, 2002

DETC2002/DAC-34131

DESIGN OPTIMIZATION FOR STRUCTURAL-ACOUSTIC PROBLEMS USING FEM-BEM

Kyung K. Choi and Jun Dong
Center for Computer-Aided Design and
Department of Mechanical & Industrial Engineering
The University of Iowa
Iowa City, IA 52242, USA
kkchoi@ccad.uiowa.edu, jundong@ccad.uiowa.edu

Nam Ho Kim
Department of Mechanical Engineering
The University of Florida
PO Box 116300
Gainesville, FL 32611-6300
nkim@ufl.edu

ABSTRACT

A structural-acoustic design optimization of a vehicle is presented using finite element and boundary element analyses. The steady-state dynamic behavior of the vehicle is calculated from the finite element frequency response analysis, while the sound pressure level within the acoustic cavity is calculated using the boundary element analysis. A reverse solution procedure is employed for the design sensitivity calculation using the adjoint variable method. An adjoint load is obtained from the acoustic boundary element re-analysis, while the adjoint solution is calculated from the structural dynamic re-analysis. The evaluation of pressure sensitivity only involves a numerical integration process for the structural part. Two design optimization problems are formulated and solved. It has been shown that the structural weight is saved when the noise level is maintained, and the weight needs to increase in order to reduce the noise level in the passenger compartment.

KEYWORDS

Structural Acoustics, Design Optimization, Finite Element Method, Boundary Element Method, Design Sensitivity Analysis

1. INTRODUCTION

The design of a comfortable vehicle increasingly draws attention to engineers according to the customer's preference. Especially, the structural-acoustic performance of a commercial vehicle becomes an important issue in the design process. The purpose of this paper is to show the feasibility of design optimization in order to minimize the vehicle's weight subjected to the structural-acoustic constraints. To arrive at this goal, the following tools are required: (1) an accurate and efficient numerical method to evaluate the structural-acoustic performance, (2) an accurate and efficient design sensitivity analysis method to calculate the gradient information, (3) constrained, nonlinear design optimization algorithm, and (4) integrated design environment in which a design engineer can efficiently work throughout multidisciplinary environment. In this paper, an example of these four important requirements is presented.

Many numerical methods have been developed to simulate the structural-acoustic performance of a commercial vehicle. The finite element method [1], the boundary element method [2], the statistical energy analysis [3,4], and the energy flow analysis [5,6,7] are a short list of developed tools. Different tools must be used based on the design interest. For example, the finite element and boundary element methods can be used for the simulation in the low-frequency ranges, while the statistical energy analysis and energy flow analysis can be used for the high-frequency ranges. In this paper, former methods are employed to simulate the vehicle's structural-acoustic performance between 1–100 Hz frequency ranges. A commercial finite element code MSC/NASTRAN [8] is used to simulate the frequency response of a vehicle structure, while a boundary element code COMET/ACOUSTICS [9] is used to calculate the sound pressure level in the cabin compartment based on the velocity information obtained from the finite element code. Such a simulation procedure is sequential and uncoupled because the vibration effect of the air does not contribute to the structural behavior.

Design sensitivity analysis (DSA) calculates the gradient information of the structural-acoustic performance with respect to the design variables, which is the panel thickness of the vehicle. Many research results [10–18] have been published in DSA of structural-acoustic problems using the finite element and boundary element methods. While the direct differentiation method in DSA follows the same solution process as the response analysis, the adjoint variable method follows a reverse process. One of the challenges of the adjoint variable method in sequential DSA is how to effectively and practically formulate

this reverse process. The opposite solution procedure in the adjoint problem causes a significant amount of inconvenience and ineffectiveness in DSA. To overcome these difficulties, a sequential adjoint variable method developed by Kim et al. [19] is used in which the adjoint load is obtained from boundary element re-analysis, and the adjoint variable is calculated from structural dynamic re-analysis.

The importance of the integrated design environment increases as many disciplines are link together during design procedure. Finite element analysis, boundary element analysis, design parameterization, design sensitivity analysis, design optimization algorithms are needed to be integrated in the design optimization of the structural-acoustic problems. The Design sensitivity analysis and optimization tool (DSO) [20] developed at the Center for Computer-Aided Design in University of Iowa is used as an integrated design environment in this paper. Graphic User Interface is provided for design engineer can perform design parameterization, structural-acoustic analysis, design sensitivity analysis, and design optimization.

The proposed sequential structural-acoustic simulation and design sensitivity analysis using adjoint variable method are applied to the optimization of a next generation concept vehicle model, by which the vehicle weight is minimized while the sound pressure level is constrained. Two design optimization problems are formulated and solved. It has been shown that the structural weight is saved when the noise level is maintained, and the weight need to increase in order to reduce the noise level in the passenger compartment.

2. STRUCTURAL-ACOUSTIC ANALYSIS

2.1 Frequency Response Analysis

The steady-state response of a structure under harmonic load $\boldsymbol{f}(\boldsymbol{x})$ with frequency ω can be written as

$$-\omega^2 \rho \boldsymbol{z}(\boldsymbol{x}) + j\omega C\boldsymbol{z}(\boldsymbol{x}) + L\boldsymbol{z}(\boldsymbol{x}) = \boldsymbol{f}(\boldsymbol{x}), \qquad \boldsymbol{x} \in \Omega^S \tag{1}$$

where Ω^S is the structure's domain, $\boldsymbol{z}(\boldsymbol{x})$ is the complex displacement, $L(\boldsymbol{x})$ is the linear partial differential operator, $\rho(\boldsymbol{x})$ is the structural mass density, and $C(\boldsymbol{x})$ is the viscous damping effect.

The variational formulation of Eq. (1) is similar to a static problem. However, since the complex variable $\boldsymbol{z}(\boldsymbol{x})$ is used for the state variable, the complex conjugate $\bar{\boldsymbol{z}}^*$ is used for the displacement variation. By multiplying Eq. (1) with $\bar{\boldsymbol{z}}^*$ and integrating it over the domain Ω^S, the variational equation can be derived after integration by parts for the differential operator L as

$$\begin{aligned} &\iint_{\Omega^S} [-\omega^2 \rho \boldsymbol{z}^T + j\omega C\boldsymbol{z}^T]\bar{\boldsymbol{z}}^* \, d\Omega^S + \iint_{\Omega^S} \boldsymbol{\sigma}(\boldsymbol{z})^T \boldsymbol{\varepsilon}(\bar{\boldsymbol{z}}^*) \, d\Omega^S \\ &\qquad = \iint_{\Omega^S} \boldsymbol{f}^{b^T} \bar{\boldsymbol{z}}^* \, d\Omega^S + \int_{\Gamma^s} \boldsymbol{f}^{s^T} \bar{\boldsymbol{z}}^* \, d\Gamma, \qquad \forall \bar{\boldsymbol{z}} \in Z \end{aligned} \tag{2}$$

where $\bar{\boldsymbol{z}}^*$ is the complex conjugate of the kinematically admissible virtual displacement $\bar{\boldsymbol{z}}$, and Z is the complex space of kinematically admissible virtual displacements. Equation (2) provides the variational equation of the dynamic frequency response under an oscillating excitation with frequency ω. For derivational convenience, the following terms are defined:

$$d_u(\boldsymbol{z}, \bar{\boldsymbol{z}}) = \iint_{\Omega^S} \rho \boldsymbol{z}^T \bar{\boldsymbol{z}}^* \, d\Omega^S \tag{3}$$

$$c_u(\boldsymbol{z}, \bar{\boldsymbol{z}}) = \iint_{\Omega^S} C\boldsymbol{z}^T \bar{\boldsymbol{z}}^* \, d\Omega^S \tag{4}$$

$$a_u(\boldsymbol{z}, \bar{\boldsymbol{z}}) = \iint_{\Omega^S} \boldsymbol{\sigma}(\boldsymbol{z})^T \boldsymbol{\varepsilon}(\bar{\boldsymbol{z}}^*) \, d\Omega^S \tag{5}$$

$$\ell_u(\bar{\boldsymbol{z}}) = \iint_{\Omega^S} \boldsymbol{f}^{b^T} \bar{\boldsymbol{z}}^* \, d\Omega^S + \int_{\Gamma^s} \boldsymbol{f}^{s^T} \bar{\boldsymbol{z}}^* \, d\Gamma \tag{6}$$

where $d_u(\bullet,\bullet)$ is the kinetic sesqui-linear form, $c_u(\bullet,\bullet)$ is the damping sesqui-linear form, $a_u(\bullet,\bullet)$ is the structural sesqui-linear form, and $\ell_u(\bullet)$ is the load semi-linear form. The definitions of the sesqui-linear and semi-linear forms can be found in Horvath [21].

Since the structure-induced pressure within the acoustic domain is related to the velocity response, it is convenient to transfer displacement to velocity using the following relation:

$$\boldsymbol{v}(\boldsymbol{x}) = j\omega \boldsymbol{z}(\boldsymbol{x}) \tag{7}$$

By using Eqs. (2)–(7), the variational equation of the frequency response problem can be obtained as

$$j\omega d_u(\boldsymbol{v}, \bar{\boldsymbol{z}}) + c_u(\boldsymbol{v}, \bar{\boldsymbol{z}}) + \frac{1}{j\omega} a_u(\boldsymbol{v}, \bar{\boldsymbol{z}}) = \ell_u(\bar{\boldsymbol{z}}), \qquad \forall \bar{\boldsymbol{z}} \in Z \tag{8}$$

The structural damping, a variant of viscous damping, is caused either by internal material friction or by the connection between structural components. It has been experimentally observed that for each cycle of vibration the dissipated energy of the material is proportional to displacement [22]. When the damping coefficient is small as in the case of structures, damping is primarily effective at those frequencies close to the resonance. The variational equation with the structural damping effect is

$$j\omega d_u(\boldsymbol{v}, \bar{\boldsymbol{z}}) + \kappa a_u(\boldsymbol{v}, \bar{\boldsymbol{z}}) = \ell_u(\bar{\boldsymbol{z}}), \qquad \forall \bar{\boldsymbol{z}} \in Z \tag{9}$$

where $\kappa = (1 + j\phi)/j\omega$, and ϕ is the structural damping coefficient.

After the structure is approximated using finite elements, and kinematic boundary conditions are applied, the following system of matrix equations is obtained:

$$[j\omega \boldsymbol{M} + \kappa \boldsymbol{K}]\{\boldsymbol{v}(\omega)\} = \{\boldsymbol{f}(\omega)\} \tag{10}$$

where $[\boldsymbol{M}]$ is the mass matrix and $[\boldsymbol{K}]$ is the stiffness matrix.

2.2 Acoustic Boundary Element Method

From the structure's velocity result, the boundary element method is used to evaluate pressure response in an acoustic domain. In the simplified forms, the boundary integral equation of the acoustic problem can be written as

$$b(\boldsymbol{x}_0; \boldsymbol{v}) + e(\boldsymbol{x}_0; p_S) = \alpha p(\boldsymbol{x}_0) \tag{11}$$

where $b(\boldsymbol{x}_0;\bullet)$ and $e(\boldsymbol{x}_0;\bullet)$ are linear integral forms that correspond to the contributions from surface velocity and surface pressure. The constant α is equal to 1 for $\boldsymbol{x}_0$ inside the acoustic

volume, 0.5 for $\boldsymbol{x}_0$ on a smooth boundary surface, and 0 for $\boldsymbol{x}_0$ outside the acoustic volume. Note that Eq. (11) can provide a solution for both radiation and interior acoustic problems. Note that unlike the structural forms in Eqs. (3)–(6), these integral forms are independent of the sizing design variable; thus no subscribed $\boldsymbol{u}$ is used in their definitions.

The boundary element method has two steps: first evaluating the pressure variable on the acoustic boundary using the structural velocity, and then calculating the pressure variable within the acoustic domain using the boundary pressure information. Let the acoustic boundary S be approximated by N number of nodes. If observation point $\boldsymbol{x}_0$ is positioned at every node, then the following linear system of equations is obtained:

$$[\boldsymbol{A}]\{\boldsymbol{p}_S\} = [\boldsymbol{B}]\{\boldsymbol{v}\} \tag{12}$$

where $\{\boldsymbol{p}_S\}=\{p_1,p_2,\ldots,p_N\}^T$ is the nodal pressure vector, $\{\boldsymbol{v}\}$ is the $3N\times1$ velocity vector, $[\boldsymbol{A}]$ is the $N\times N$ coefficient matrix, and $[\boldsymbol{B}]$ is the $N\times3N$ coefficient matrix. Note that these vectors and matrices are all complex variables. The process of computing the boundary pressure $\{\boldsymbol{p}_S\}$ assumes domain discretization, and the condition in Eq. (11) is imposed in every node. However, for the purposes of DSA, let us consider a continuous counterpart to Eq. (12), defined as

$$A(\boldsymbol{p}_S) = B(\boldsymbol{v}) \tag{13}$$

where the integral forms $A(\bullet)$ and $B(\bullet)$ correspond to the matrices $[\boldsymbol{A}]$ and $[\boldsymbol{B}]$ in Eq. (12), respectively. The boundary pressure can then be calculated from $p_S = A^{-1}\circ B(\boldsymbol{v})$.

Once $\{\boldsymbol{p}_S\}$ has been computed, Eq. (11) can be used to compute the acoustic pressure at any point $\boldsymbol{x}_0$ within the acoustic domain in the form of a vector equation as

$$p(\boldsymbol{x}_0) = \{\boldsymbol{b}(\boldsymbol{x}_0)\}^T\{\boldsymbol{v}\} + \{\boldsymbol{e}(\boldsymbol{x}_0)\}^T\{\boldsymbol{p}_S\} \tag{14}$$

where $\{\boldsymbol{b}(\boldsymbol{x}_0)\}$ and $\{\boldsymbol{e}(\boldsymbol{x}_0)\}$ are the column vectors that correspond to the left-hand side of the boundary integral Eq. (11).

In the sizing design problem, in which panel thickness is a design variable, integral forms $b(\boldsymbol{x}_0;\bullet)$ and $e(\boldsymbol{x}_0;\bullet)$ in Eq. (11) are independent of the design variable. Only implicit dependence on the design exists through the state variable $\boldsymbol{v}$ and p, which will be developed in the following section. However, in the shape design problem, the acoustic domain changes according to the structural domain change, which is a design variable. Thus, integral forms $b(\boldsymbol{x}_0;\bullet)$ and $e(\boldsymbol{x}_0;\bullet)$ depend on the design.

3. DESIGN SENSITIVITY ANALYSIS

The purpose of design sensitivity analysis (DSA) is to compute the dependency of performance measures on the design. In this study, only sizing design is considered, such as the thickness of a plate and the cross-sectional dimension of a beam.

3.1 Direct Differentiation Method

A direct differentiation method computes the variation of state variables by differentiating the state Eqs. (9) and (11) with respect to the design. Let us first consider the structural part, i.e., the frequency response analysis in Eq. (9). The forms that appear in Eq. (9) explicitly depend on the design, and their variations are defined as

$$d'_{\delta\boldsymbol{u}}(\boldsymbol{v},\bar{\boldsymbol{z}}) \equiv \frac{d}{d\tau}[d_{\boldsymbol{u}+\tau\delta\boldsymbol{u}}(\tilde{\boldsymbol{v}},\bar{\boldsymbol{z}})]\bigg|_{\tau=0} \tag{15}$$

$$a'_{\delta\boldsymbol{u}}(\boldsymbol{v},\bar{\boldsymbol{z}}) \equiv \frac{d}{d\tau}[a_{\boldsymbol{u}+\tau\delta\boldsymbol{u}}(\tilde{\boldsymbol{v}},\bar{\boldsymbol{z}})]\bigg|_{\tau=0} \tag{16}$$

$$\ell'_{\delta\boldsymbol{u}}(\bar{\boldsymbol{z}}) \equiv \frac{d}{d\tau}[\ell_{\boldsymbol{u}+\tau\delta\boldsymbol{u}}(\bar{\boldsymbol{z}})]\bigg|_{\tau=0} \tag{17}$$

where $\tilde{\boldsymbol{v}}$ denotes state variable $\boldsymbol{v}$ with the dependence on τ being suppressed, and $\bar{\boldsymbol{z}}$ and its complex conjugate are independent of the design. The detailed expressions of $d'_{\delta\boldsymbol{u}}(\bullet,\bullet)$, $a'_{\delta\boldsymbol{u}}(\bullet,\bullet)$, and $\ell'_{\delta\boldsymbol{u}}(\bullet)$ can be found in Kim et al. [19].

Thus, by taking a variation of both sides of Eq. (9) with respect to the design, and by moving terms explicitly dependent on the design to the right side, the following sensitivity equation can be obtained:

$$\begin{aligned} &j\omega d_{\boldsymbol{u}}(\boldsymbol{v}',\bar{\boldsymbol{z}}) + \kappa a_{\boldsymbol{u}}(\boldsymbol{v}',\bar{\boldsymbol{z}}) \\ &\quad = \ell'_{\delta\boldsymbol{u}}(\bar{\boldsymbol{z}}) - j\omega d'_{\delta\boldsymbol{u}}(\boldsymbol{v},\bar{\boldsymbol{z}}) - \kappa a'_{\delta\boldsymbol{u}}(\boldsymbol{v},\bar{\boldsymbol{z}}), \qquad \forall\bar{\boldsymbol{z}}\in Z \end{aligned} \tag{18}$$

Presuming that the velocity $\boldsymbol{v}$ is given as a solution to Eq. (9), Eq. (18) is a variational equation, with the same sesqui-linear forms for displacement variation $\boldsymbol{v}'$. Note that the stiffness matrices corresponding to Eqs. (9) and (18) are the same, and that the right side of Eq. (18) can be considered a fictitious load term. If a design perturbation $\delta\boldsymbol{u}$ is defined, and if the right side of Eq. (18) is evaluated with the solution of Eq. (9), then Eq. (18) can be numerically solved to obtain $\boldsymbol{v}'$ using the finite element method. By interpreting the right side of Eq. (18) as another load form, Eq. (18) can be solved by using the same solution process as the frequency response problem in Eq. (9).

Now the acoustic aspect will be considered, which is represented by the boundary integral Eq. (11). A direct differentiation of Eq. (11) yields the following sensitivity equation:

$$b(\boldsymbol{x}_0;\boldsymbol{v}') + e(\boldsymbol{x}_0;\, p'_S) = \alpha p'(\boldsymbol{x}_0) \tag{19}$$

Since integral forms $b(\boldsymbol{x}_0;\,\bullet)$ and $e(\boldsymbol{x}_0;\,\bullet)$ are independent of the design, the above equation has exactly the same form as Eq. (11) . Thus, using the solution ($\boldsymbol{v}'$) of the structural sensitivity Eq. (18), Eq. (19) can be used by following the same solution process as BEM, to obtain the pressure sensitivity result. Thus, like Eq. (12), the following matrix equation has to be solved in the discrete system:

$$[\boldsymbol{A}]\{\boldsymbol{p}'_S\} = [\boldsymbol{B}]\{\boldsymbol{v}'\} \tag{20}$$

Then, like Eq. (14), the pressure sensitivity at point $\boldsymbol{x}_0$ can be obtained from

$$p'(\boldsymbol{x}_0) = \{\boldsymbol{b}(\boldsymbol{x}_0)\}^T\{\boldsymbol{v}'\} + \{\boldsymbol{e}(\boldsymbol{x}_0)\}^T\{\boldsymbol{p}'_S\} \tag{21}$$

This sensitivity calculation process is the same as the BEM solution process described from Eq. (12) to Eq. (14).

Consider a performance measure that is defined at point $\boldsymbol{x}_0$ within the acoustic domain as

$$\psi(\boldsymbol{x}_0) = h\big(p(\boldsymbol{x}_0), \boldsymbol{u}\big) \tag{22}$$

where the function $h(p,\boldsymbol{u})$ is assumed to be continuously differentiable with respect to its arguments. The variation of the performance measure with respect to the design variable becomes

$$\begin{aligned}\psi' &= \frac{d}{d\tau}\big[h(p(\boldsymbol{x};\boldsymbol{u}+\tau\delta\boldsymbol{u}), \boldsymbol{u}+\tau\delta\boldsymbol{u})\big]\Big|_{\tau=0} \\ &= h_{,p}\, p' + h_{,\boldsymbol{u}}^T \delta\boldsymbol{u}\end{aligned} \tag{23}$$

where the expression of $h_{,p}=\partial h/\partial p$ and $h_{,\boldsymbol{u}}=\partial h/\partial \boldsymbol{u}$ are known from the definition of the function h. Thus, from the solution to the acoustic design sensitivity Eq. (19), the sensitivity of ψ can readily be calculated. However, the calculation of p' also requires the solution to the structural sensitivity Eq. (18).

3.2 Adjoint Variable Method

Since the number of design variables is larger than the number of active constraints in many optimization problems, the adjoint variable method is attractive. However, the adjoint variable method is known to be limited to a symmetric operator problem. In this section, the adjoint variable method is further extended to non-symmetric complex operator problems. Since the adjoint variable method is directly related to the performance measure, structural and acoustic performance measures are treated separately. In case of an acoustic performance measure, a sequential adjoint variable method is introduced.

Acoustic performance ψ in Eq. (22) is defined at point $\boldsymbol{x}_0$, and its sensitivity expression in Eq. (23) contains p', which has to be explicitly expressed in terms of $\delta\boldsymbol{u}$. The objective is to express p' in terms of $\boldsymbol{v}'$ such that the adjoint problem defined in the previous section can be used. By substituting the relation in Eq. (19) into the sensitivity expression of Eq. (23), and by using the relation in Eq. (13), we obtain

$$\begin{aligned}\psi' &= h_{,\boldsymbol{u}}^T \delta\boldsymbol{u} + h_{,p}\, p' \\ &= h_{,\boldsymbol{u}}^T \delta\boldsymbol{u} + h_{,p}[b(\boldsymbol{x}_0;\boldsymbol{v}') + e(\boldsymbol{x}_0; A^{-1}\circ B(\boldsymbol{v}'))]\end{aligned} \tag{24}$$

In Eq. (24), α=1 is used since $\boldsymbol{x}_0$ is the interior point. Thus, ψ' is expressed in terms of $\boldsymbol{v}'$. The second term on the right side of the above equation can be used to define the adjoint load by substituting $\bar{\lambda}$ for $\boldsymbol{v}'$. Hence, the following form of the adjoint problem is obtained:

$$\begin{aligned}&j\omega d_{\boldsymbol{u}}(\bar{\lambda}, \lambda) + \kappa a_{\boldsymbol{u}}(\bar{\lambda}, \lambda) \\ &\qquad = h_{,p}[b(\boldsymbol{x}_0;\bar{\lambda}) + e(\boldsymbol{x}_0; A^{-1}\circ B(\bar{\lambda}))], \qquad \forall \bar{\lambda} \in Z\end{aligned} \tag{25}$$

where an adjoint solution λ^* is desired. After calculating λ^*, the sensitivity of ψ can be obtained as

$$\psi' = h_{,\boldsymbol{u}}\delta\boldsymbol{u} + \ell'_{\delta\boldsymbol{u}}(\lambda) - j\omega d'_{\delta\boldsymbol{u}}(\boldsymbol{v}, \lambda) - \kappa a'_{\delta\boldsymbol{u}}(\boldsymbol{v}, \lambda) \tag{26}$$

It is interesting to note that even if ψ is a function of pressure p, its sensitivity expression in Eq. (26) does not require the value of p; only the structural solution $\boldsymbol{v}$ and the adjoint solution λ^* are required in the calculation of ψ'.

Consider a discrete form of the adjoint load. Equation (25) can be written in the discrete system as

$$[j\omega\boldsymbol{M} + \kappa\boldsymbol{K}]\{\lambda^*\} = \{\boldsymbol{b}\} + [\boldsymbol{B}]^T[\boldsymbol{A}]^{-T}\{\boldsymbol{e}\} \tag{27}$$

where the right side corresponds to the adjoint load in the discrete system. Instead of computing the inverse matrix, let us define an acoustic adjoint problem in BEM as

$$[\boldsymbol{A}]^T\{\boldsymbol{\eta}\} = \{\boldsymbol{e}\} \tag{28}$$

where the acoustic adjoint solution $\{\boldsymbol{\eta}\}$ is desired. Even though the coefficient matrix $[\boldsymbol{A}]$ is not symmetric, the adjoint Eq. (28) can still use the factorized matrix of the boundary element Eq. (12). By substituting $\{\boldsymbol{\eta}\}$ into Eq. (27), we obtain the structural adjoint problem as

$$[j\omega\boldsymbol{M} + \kappa\boldsymbol{K}]\{\lambda^*\} = \{\boldsymbol{b}\} + [\boldsymbol{B}]^T\{\boldsymbol{\eta}\} \tag{29}$$

Note that the acoustic adjoint solution $\{\boldsymbol{\eta}\}$, which is obtained from BEM, is required to compute the structural adjoint load, and frequency response re-analysis then provides the structural adjoint solution $\{\lambda^*\}$. Thus, two different adjoint problems are defined: the first is similar to BEM, and is used to compute the adjoint load, while the second is similar to the structural frequency-response problem.

3.3 Numerical Methods

A structural-acoustic system is solved using both finite element and the boundary element methods. The variational equation of the harmonic motion of a continuum model, Eq. (9), can be reduced to a set of linear algebraic equations by discretizing the model into elements and by introducing shape functions and nodal variables for each element. It is assumed that the structural finite element and the acoustic boundary element meshes match at their interfaces. Acoustic pressure $p(\boldsymbol{x})$ and structural velocity $\boldsymbol{v}(\boldsymbol{x})$ are approximated using shape functions and nodal variables for each element in the discretized model as

$$\left.\begin{aligned}\boldsymbol{v}(\boldsymbol{x}) &= \boldsymbol{N}_s(\boldsymbol{x})\boldsymbol{v}^e \\ p(\boldsymbol{x}) &= \boldsymbol{N}_a(\boldsymbol{x})\boldsymbol{p}^e\end{aligned}\right\} \tag{30}$$

where $N_s(\boldsymbol{x})$ and $N_a(\boldsymbol{x})$ are matrices of shape functions for velocity and pressure, respectively, and $\boldsymbol{v}^e$ and $\boldsymbol{p}^e$ are the element nodal variable vectors. Substituting Eq. (30) into Eq. (9) and carrying out integration yields the same matrix equation as Eq. (10), rewritten here

$$[j\omega\boldsymbol{M} + \kappa\boldsymbol{K}]\{\boldsymbol{v}(\omega)\} = \{\boldsymbol{f}(\omega)\} \tag{31}$$

After obtaining the structural velocity, BEM is used to evaluate the pressure response on the boundary, as well as within the acoustic domain, as explained in Section 2.2.

Part of Figure 1 shows the computational procedure for the adjoint variable method with a structural FEA and an acoustic

BEA code. Even if FEM and BEM are used to evaluate the acoustic performance measure, only structural response $\boldsymbol{v}$ is required to perform design sensitivity analysis. The adjoint load is calculated from the transposed boundary element analysis, and the adjoint equations are then numerically solved using the FEA code with the same finite element model used for the original structural analysis.

Numerical solutions are used to compute the design sensitivity, and the integration of the design sensitivity expressions in Eq. (26) can be evaluated using a numerical integration method, such as the Gauss quadrature method [1]. The integrands are functions of the state variable, the adjoint variable, and gradients of both variables, as illustrated in Eq. (26).

4. DESIGN OPTIMIZATION

For structural-acoustic problem, the sequential FEM-BEM analysis calculates the performance measure (noise and vibration), and the adjoint variable method for DSA calculates the sensitivity of the performance measure. These information are utilized by the optimization program to search for the optimum design.

4.1 Optimization Procedure for a Sequential Structural-Acoustic Problem

Gradient-based optimization algorithms are commonly used in engineering design and optimization. The performance measure and its sensitivity are required for the gradient-based optimization process. Figure 1 shows the computational procedure for the optimization of sequential structural-acoustic problem using gradient-based optimization algorithms. Once design variable, cost function and design constraint are defined, the proposed FEM-BEM sequential analysis and adjoint variable DSA method are employed to compute the performance measure and its sensitivity, which will be input to the optimization to search for the optimum design. The whole process will loop until an optimum design is achieved.

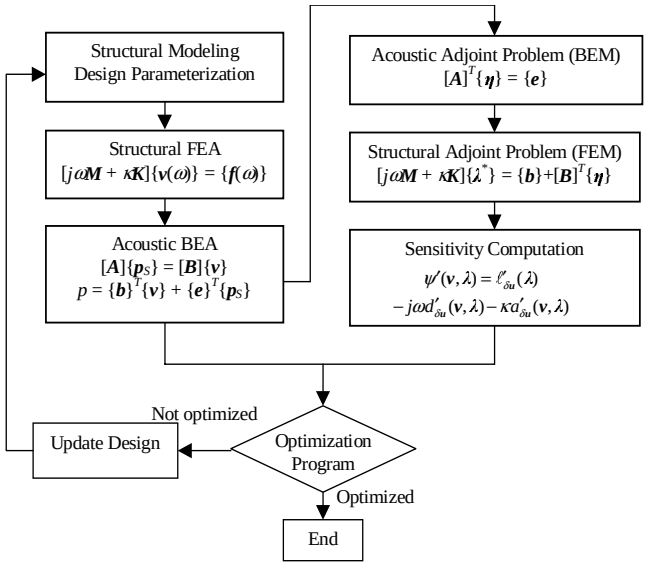

Figure 1. Computational Procedure of FEM-BEM Optimization

4.2 Numerical Example—NVH Optimization of a Vehicle

One of important applications of the proposed method is structure-borne noise reduction of the commercial vehicle. Figure 2 shows concept design finite element and boundary element models of a next generation hydraulic hybrid vehicle [19]. In addition to power-train vibration and wheel/terrain interaction, a hydraulic pump is a source of vibration, considered as a harmonic excitation. Because of this additional source of excitation, vibration and noise is more significant than that with a conventional power train. The object of the design optimization is to minimize the vehicle weight as well as keeping the lowest noise and vibration level at the driver's position.

From the power train analysis and rigid-body dynamic analysis, the harmonic excitations at twelve locations are obtained. Frequency response analysis is carried out on the structural FE model using MSC/NASTRAN to obtain the velocity response, which correspond to the structure's natural frequencies below 100 Hz. COMET/Acoustic [9] is employed as the BEA code to obtain the acoustic pressure performance on the acoustic BEA model which is also shown in Figure 2. Once the acoustic performance measure and sensitivity information are both obtained according to the procedure illustrated in Figure 1, DOT (Design Optimization Tool) [20] is applied as the optimization program and sequential quadratic programming algorithm is used to search for the optimum design.

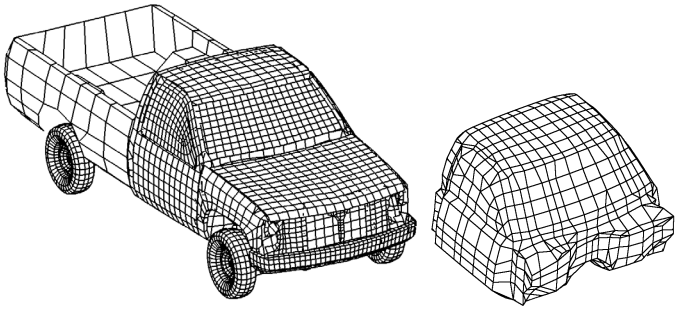

Figure 2. Vehicle Structure FE Model and Acoustic BE Model of the Cabin Part

4.2.1 FEM-BEM Analysis and Design Sensitivity Analysis of the Vehicle Model

The sequential FEM-BEM analysis is performed on the vehicle FEA and BEA models. In this example, the noise level of the passenger compartment is chosen as the performance measure, and vehicle panel thicknesses are chosen as design variables. The sound pressure levels at the driver's ear position is obtained and shown in Table 1.

Table 1. Sound Pressure Levels at Driver's Ear Position

Frequency (Hz)	Pressure (kg/mm·sec^2)	Phase Angle (Degree)
47.3	0.64275E–04	66.915
59.5	0.35889E–03	328.99
75.9	0.66052E–04	193.91
81.8	0.41081E–03	264.21
86.0	0.21629E–03	176.18
90.5	0.43862E–03	171.44
94.0	0.75627E–02	178.30
98.7	0.22676E–03	226.07

Since the sound pressure level at 94.0 Hz is significantly higher than those at other frequencies, design modification will be carried out mainly around that frequency. Figure 3 shows the sound pressure level inside the cabin compartment. The sound pressure level at the driver's ear position is 74.58 dB.

Forty design variables are selected in this example. First, the acoustic adjoint problem in Eq. (28) is solved, and the structural adjoint problem of Eq. (29) is then solved to obtain the adjoint response λ^*. Using velocity response $\boldsymbol{v}$ and adjoint response λ^*, the numerical integration process calculates the sensitivity results for each structural panel, as shown in Table 2. The sensitivity contribution from each panel is normalized in order to show the relative magnitude of design sensitivity. The results show that a thickness change in the chassis component has the greatest potential for achieving a reduction in sound pressure levels. Since the numerical integration process is carried out on each finite element, the element sensitivity information can be calculated without any additional effort. Figure 4 plots the sensitivity contribution of the each element to the sound pressure level. Such graphic-based sensitivity information is very helpful for the design engineer to determine the direction of the design modification.

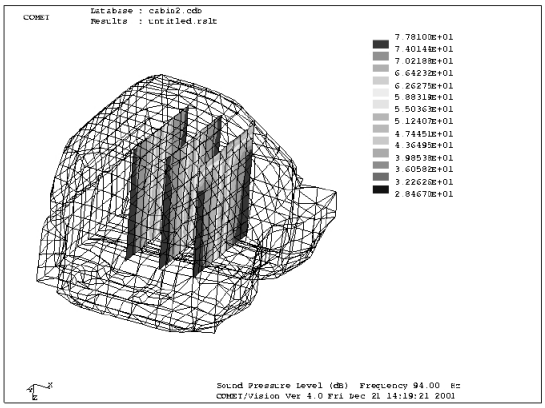

Figure 3. Sound Pressure Plot at Driver's Position (Max:77.8 dB)

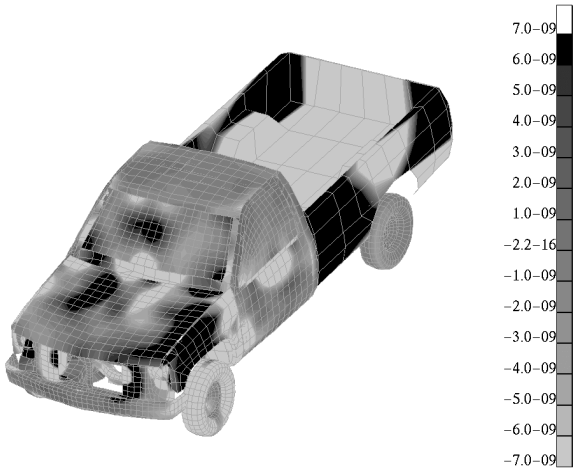

Figure 4. Element Design Sensitivity Plot w.r.t. Panel Thickness

Table 2. Normalized Sound Pressure Sensitivity w.r.t. Panel Thickness

Component	Sensitivity	Component	Sensitivity
Chassis	–1.0	Chassis MTG	–0.11
Left wheelhouse	–0.82	Chassis connectors	–0.10
Right door	0.73	Right fender	–0.07
Cabin	–0.35	Left door	–0.06
Right wheelhouse	–0.25	Bumper	–0.03
Bed	–0.19	Rear glass	0.03

4.2.2 Optimization of the Vehicle Model—Case 1

The first design problem is to find whether the vehicle weight can be reduced while maintaining the noise level in the driver's ear position with the initial vehicle. Therefore, the

weight (mass) of the vehicle is chosen as the objective function, and the sound pressure level in the driver's ear position is chosen as a design constraint. The maximum value of the sound pressure 74.58 dB in the initial design is used for the constraint boundary.

Although, the maximum sound pressure appears at 94 Hz in the initial design, the frequency that has the maximum pressure may shift during design process because of design change. However, it is difficult to constrain all continuous frequency ranges. Thus, a fixed set of discrete frequencies is chosen in order to evaluate sound pressure level. Since five resonant frequencies exist between frequency 80 and 100 Hz as shown in Table 1, a total of eleven equally distributed frequencies between 80 and 100 Hz are chosen to evaluate the sound pressure level during design optimization.

Although forty design variables are used to calculate design sensitivity information, ten design variables are allowed to change during design optimization because some of panel thicknesses are difficult to change for design purposes and some of them are related to the vehicle's performance. Ten design variables are panel thicknesses of Chassis, Fender-Left, Fender-Right, Wheelhouse-Left, Wheelhouse-Right, Cabin, Door-Left, Door-Right, Chassis-Conn, and Chassis-MTG, which significantly contribute to the sound and vibration level inside the cabin and are easy to change for design purposes. Accordingly, the design optimization problem can be defined as

Minimize Cost Function $c(\boldsymbol{u})$ = mass
Subject to Design Constraints $g_i = p(\boldsymbol{u}, f_i) - 74.58 \leq 0$, $i = 1,\ldots, 11$

f_i = 80, 82, …, 100 Hz
Design Variables: $\boldsymbol{u} = [h_1, h_2, \ldots, h_{10}]^T$

The design optimization procedure illustrated in Figure 5 is carried out. A seamless integration between FEM, BEM, sensitivity module, and optimization module are critical in automated design process. MSC/NASTRAN is used for finite element frequency response analysis, while COMET/Acoustic is used for the acoustic boundary element analysis. Design sensitivity information is calculated from design sensitivity and optimization tool (DSO). A sequential programming algorithm in the commercial optimization program DOT is used for design optimization. The design optimization problem is converged after nine iterations. A total of 27 response analyses and nine design sensitivity analyses have been used during design optimization. Table 3 compares the design variables between initial and optimum designs. All design variables are reduced to reach the optimum design because the design constraints in the initial design are feasible.

Table 3. Optimum Design Result (Case 1)

Design Variable	Initial Design	Optimum Design
x_1 (Chassis)	3.137	2.51187
x_2 (Fender-Left)	0.8	0.666085
x_3 (Fender-Right)	0.8	0.667751
x_4 (Wheelhouse-Left)	0.696	0.650193
x_5 (Wheelhouse-Right)	0.696	0.556948
x_6 (Cabin)	2.5	2.0
x_7 (Door-Left)	1.24	0.992068
x_8 (Door-Right)	1.24	0.993665
x_9 (Chassis-Conn)	3.611	2.88888
x_{10} (Chassis-MTG)	3.0	2.4

Table 4. History of Cost Function and Constraint (Case 1)

History	Cost Function (Mass, ton)	Design Constraint (dB) f = 94 Hz
Initial Design	1.705834	74.580
Iteration 1	1.659714	79.191
Iteration 2	1.667589	75.693
Iteration 3	1.681121	75.531
Iteration 4	1.640682	68.900
Iteration 5	1.639878	73.385
Iteration 6	1.636071	74.484
Iteration 7	1.628628	67.277
Iteration 8	1.628073	74.568
Iteration 9 (Optimum)	1.628072	74.579

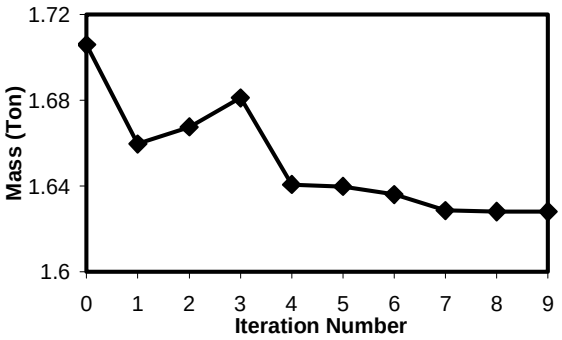

Figure 5. Cost Function History (Case 1)

Table 4 and Figure 5 show the history of the cost function. The total mass of the vehicle decreases from 1,705.834 Kg to 1,628.072 Kg, which reduces 77.762 Kg. The structural mass significantly decreases in the first iteration, which violates the noise level constraint. Thus, the next three iterations are used to recover the constraint violation. The structural mass is also noticeably decreases at the fourth iteration. At the optimum design, the noise and vibration maintains the same level as the initial design.

Figure 6 shows the sound pressure distribution inside the cabin compartment before and after optimization. Even if design variables are changed more than 20% from the initial design, the design optimization algorithm choose the layout of panel

thicknesses such that the sound pressure distribution in the cabin compartment is almost the same with the initial design.

The optimization results explain that the initial design is not an optimum in the NVH design point of view. Using the FEM-BEM analysis and the proposed adjoint variable DSA methods combined with the optimization program, it is proved that the total vehicle weight can be reduced, while the noise and vibration level still remain the same as the initial design.

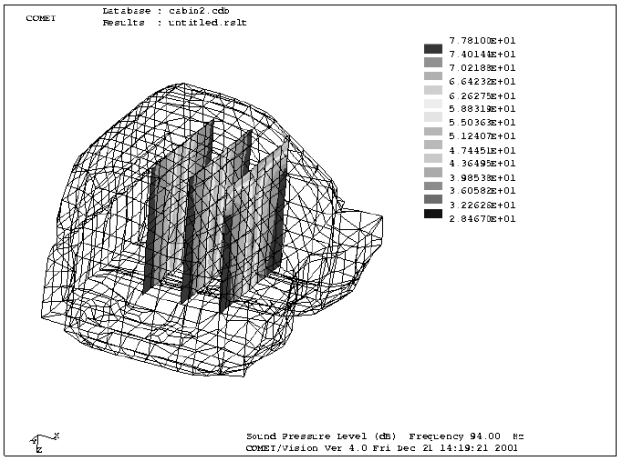

(a) Initial Design

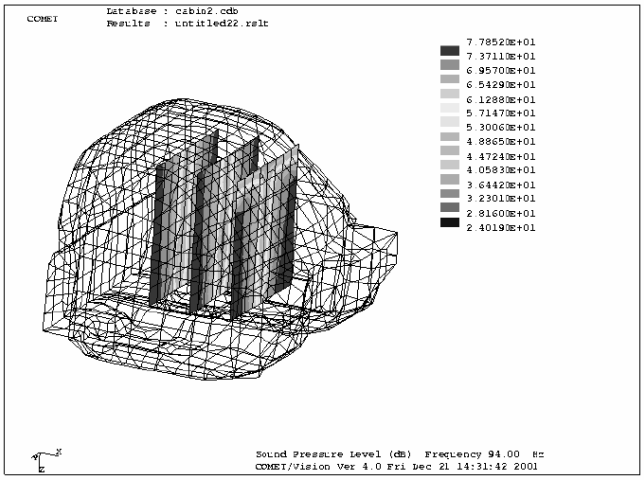

(b) Optimum Design

Figure 6. Acoustic Pressure Distribution Inside Cabin

Figure 7 shows the change of the sound pressure level at driver's ear position in the frequency range from 80 to 100 Hz during the optimization process. Although the noise distribution in this frequency range changes due to the design change, the peak noise level during the total frequency range will remain the same such that the design constraints will not be violated. Note that the frequency in which the maximum sound pressure appears does not change from 94 Hz. This is because 94 Hz is the acoustic natural frequency of the internal cabin. Since the panel thickness design does not change the cabin geometry, the acoustic natural frequency remains constant.

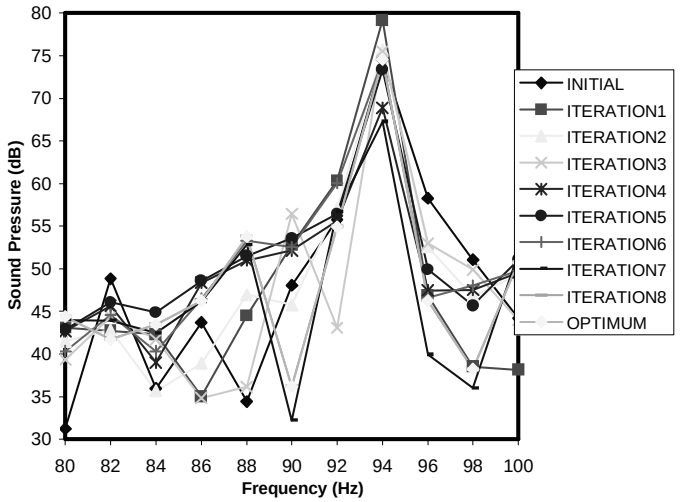

Figure 7. Design Constraints History in the Frequency Range between 80 and 100 Hz (Case 1)

4.2.3 Optimization of the Vehicle Model—Case 2

The second optimization example is to minimize the vehicle weight while reducing the noise and vibration level inside the cabin compartment. Therefore, compared with the design optimization case 1, the difference is the limit value of the design constraints. In order to reduce the noise level, a new limit value 66 dB of the design constraint is chosen for the optimization problem at driver's ear position, which indicates more than 60% decrease of noise level. The design variables and objection function will still be the same as Case 1. Thus, the design optimization problem is defined as

Minimize Cost Function $c(\boldsymbol{u})$ = mass
Subject to Design Constraints $g_i = p(\boldsymbol{u}, f_i) - 66.0 \leq 0$, $i = 1,\ldots, 11$

f_i = 80, 82, …, 100 Hz
Design Variables: $\boldsymbol{u} = [h_1, h_2, \ldots, h_{10}]^T$

In Case 2, the design optimization problem is converged in five iterations. Since the current design is infeasible, the optimization algorithm increases all design variables to satisfy constraint violation. After the first iteration, the constraint violation is removed, and the optimization algorithm is converged within a feasible region to find the optimum design. Optimization results show that the design variables need to be increased to satisfy the design constraints. Table 5 compares the initial and optimum values of design variables. All ten panel thicknesses have been increased at the optimum design.

Table 6 and Figure 8 show the design history of the cost function, which increases from 1,705.834 Kg to 1,762.132 Kg, totally increasing 56.298 Kg. However, the noise and vibration

level of the vehicle significantly decrease compared to the initial design.

Table 5. Optimum Design Result (Case 2)

Design Variable	Initial Design	Optimum Design
x_1 (Chassis)	3.137	3.63889
x_2 (Fender-Left)	0.8	0.944577
x_3 (Fender-Right)	0.8	0.944569
x_4 (Wheelhouse-Left)	0.696	0.822522
x_5 (Wheelhouse-Right)	0.696	0.822288
x_6 (Cabin)	2.5	2.8014
x_7 (Door-Left)	1.24	1.46084
x_8 (Door-Right)	1.24	1.46131
x_9 (Chassis -Conn)	3.611	4.24012
x_{10} (Chassis -MTG)	3.0	3.53968

Table 6. History of Cost Function and Constraint (Case 2)

History	Cost Function (Mass, ton)	Design Constraint (dB) f = 94 Hz
Initial Design	1.705834	74.58
Iteration 1	1.780957	65.525
Iteration 2	1.776322	65.252
Iteration 3	1.762217	65.997
Iteration 4	1.762132	66.006
Iteration 5 (Optimum)	1.762132	66.006

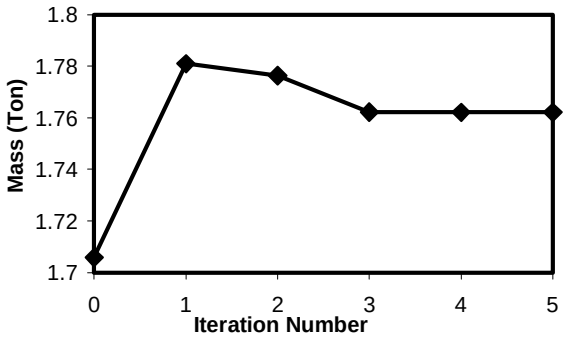

Figure 8. Cost Function History (Case 2)

Figure 9 shows the sound pressure distribution inside the cabin compartment before and after optimization. Different from Case 1, the internal sound pressure distribution is quite different between initial and optimum designs.

Figure 10 shows the change of the sound pressure level at driver's ear position in the frequency range from 80 to 100 Hz during the optimization process. Although the total vehicle weight increases, the noise distribution in the frequency range will decrease significantly due to the design change.

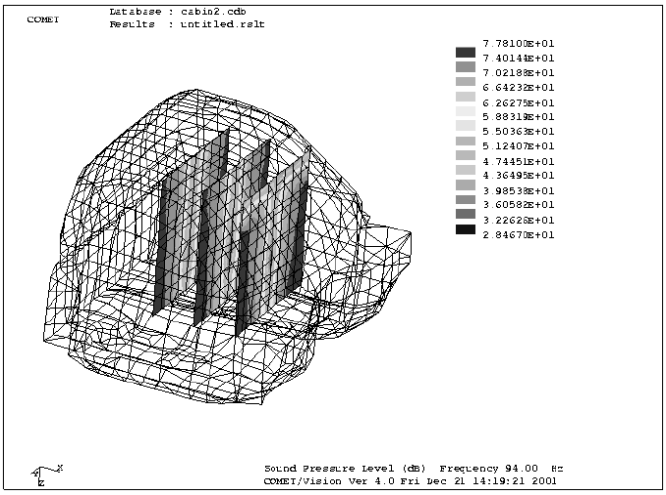

(a) Initial Design

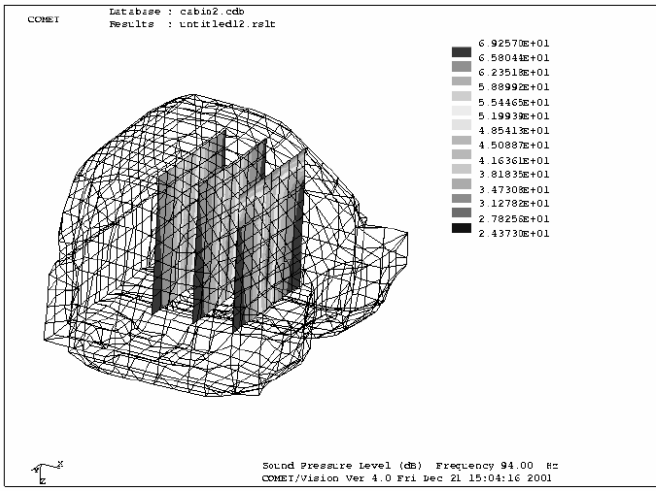

(b) Optimum Design

Figure 9. Acoustic Pressure Distribution Inside Cabin

5. CONCLUSIONS

Based on the assumption that acoustic behavior does not influence structural behavior, design sensitivity analysis and optimization of a sequential structural-acoustic problem is presented using FEM-BEM. In the adjoint variable method, a sequential adjoint problem is presented in which the adjoint load is calculated by solving a boundary adjoint problem and the adjoint solution is calculated from a structural adjoint problem. Design optimization based on the sequential FEM-BEM analysis and adjoint variable DSA method is carried out on a concept vehicle structure with satisfactory results. Depending on the design problem definition, different design optimization results are observed.

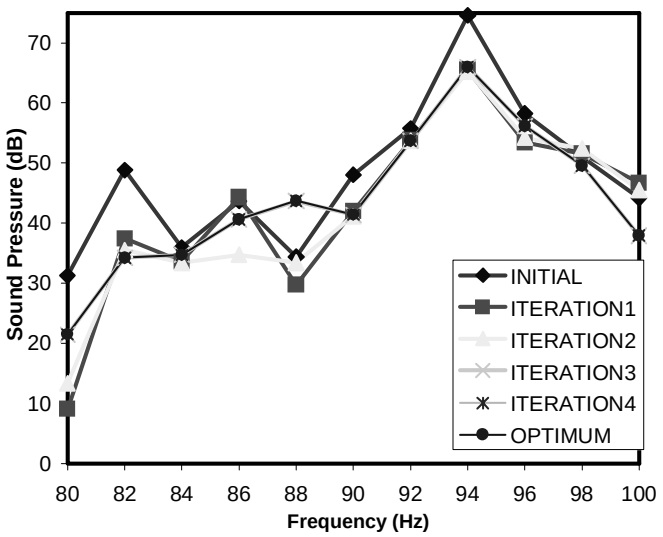

Figure 10. Design Constraints History in the Frequency Range between 80 and 100 Hz (Case 2)

ACKNOWLEDGEMENTS

This research is supported by the Automotive Research Center that is sponsored by the US Army TARDEC under contract DAAE07-94-C-R094. The authors sincerely appreciate Profs. C. Pierre and N. Vlahopoulos, and Drs. Z.D. Ma and M. Castanier for their truck model and collaboration in ARC research for this research.

REFERENCES

[1] Hughes, T. J. R., 1987, The Finite Element Method. Prentice-Hall, Englewood Cliffs, NJ.

[2] Kythe, P. K., 1995, Introduction to Boundary Element Methods. CRS Press, Florida.

[3] Lyon, R., 1975, Statistical Energy Analysis of Dynamical Systems: Theory and Application, The MIT Press, Cambridge, MA

[4] Rybak, S. A., 1972, Waves in Plate Containing Random Inhomogeneities, Soviet Physics and Acoustics **17**(3) 345–349

[5] Nefske, D. J. and Sung, S. H., 1989, Power Flow Finite–Element Analysis of Dynamic–Systems – Basic Theory and Application to Beams, Journal of Vibration Acoustics Stress and Reliability in Design **111**(1) 94–100

[6] R. J. Bernhard and J. E. Huff, 1999, Structural–Acoustic Design at High Frequency Using the Energy Finite Element Method, Journal of Vibration and Acoustics **121**(3) 295–301

[7] N. Vlahopoulos, L. O. Garza-Rios, and C. Mollo, 1999, Numerical Implementation, Validation, and Marine Applications of an Energy Finite Element Formulation, Journal of Ship Research **43**(3) 143–156

[8] Gockel, M. A., 1983, MSC/NASTRAN Handbook for Dynamic Analysis. The MacNeal-Schwendler Corporation, 815 Colorado Blvd., Los Angeles, CA.

[9] COMET/ACOUSTIC User's Manual, Automated Analysis Corporation

[10] Ma, Z. -D., and Hagiwara, I., 1991, "Sensitivity analysis-method for coupled acoustic-structural systems Part 2: direct frequency-response and its sensitivities," AIAA Journal, 29, pp. 1796-1801.

[11] Choi, K. K., Shim, I., and Wang, S., 1997, "Design sensitivity analysis of structure-induced noise and vibration," Journal of Vibration and Acoustics, 119, pp. 173-179.

[12] Nefske, D. J., Wolf, J. A., and Howell, L. J., 1982, "Structural-acoustic finite element analysis of the automobile passenger compartment: A review of current practice," Journal of Sound and Vibration, 80, pp. 247-266.

[13] Salagame, R. R., Belegundu, A. D., and Koopman, G. H., 1995, "Analytical sensitivity of acoustic power radiated from plates," Journal of Vibration and Acoustics, 117, pp. 43-48.

[14] Scarpa, F., 2000, "Parametric sensitivity analysis of coupled acoustic-structural systems," Journal of Vibration and Acoustics, 122, pp. 109-115.

[15] Smith, D. C., and Bernhard, R. J., 1992, "Computation of acoustic shape design sensitivity using a boundary element method," Journal of Vibration and Acoustics, 114, pp. 127-132.

[16] Cunefare K. A., and Koopman, G. H., 1992, "Acoustic design sensitivity for structural radiators," Journal of Vibration and Acoustics, 114, pp. 179-186.

[17] Kane, J. H., Mao, S., and Everstine, G. C., 1991, "Boundary element formulation for acoustic shape sensitivity analysis," Journal of the Acoustical Society of America, 90, pp. 561-573.

[18] Matsumoto, T., Tanaka, M., and Yamada, Y., 1995, "Design sensitivity analysis of steady-state acoustic problems using boundary integral equation formulation," JSME International Journal Series C, 38, pp. 9-16.

[19] Kim, N.H., Choi, K.K., Dong, J., Pierre, C., Vlahopoulos, N., Ma, Z.D., Castanier, M., "A Sequential Adjoint Variable Method in Design Sensitivity Analysis of NVH Problems," ASME International Mechanical Engineering Congress and Exposition (IMECE'01), November 11-16, 2001, New York, NY.

[20] Chang, K. H., K. K. Choi, C. S. Tsai, C. J. Chen, B. S. Choi, and X. Yu. 1995. "Design Sensitivity Analysis and Optimization Tool (DSO) for Shape Design Applications," *Computing Systems in Engineering*, 6(2):151–175.

[21] Horvath, J., 1966, Topological vector spaces and distributions. Addison-Wesley, London.

[22] Dimarogonas, A. D., 1976, Vibration Engineering. West Publishing Co.